A scalable homeostatic memory model using structural plasticity

Building a realistic, scalable memory model with independent engrams using a homeostatic mechanism

Marvin Kaster[1*], Fabian Czappa[1], Markus Butz-Ostendorf[1], Felix Wolf[1]

1 Technische Universität Darmstadt, Department of Computer Science, Laboratory for Parallel Programming, Germany

* marvin.kaster@tu-darmstadt.de

Abstract

Memory formation is usually associated with Hebbian learning, using synaptic plasticity to change the synaptic strengths but omitting structural changes. Recent work suggests that structural plasticity can also lead to silent memory engrams, reproducing a conditioned learning paradigm with neuron ensembles. However, this work is limited by its way of synapse formation, enabling the formation of only one memory engram. Overcoming this, our model allows the formation of many engrams simultaneously while retaining high neurophysiological accuracy, e.g., as found in cortical columns. We achieve this by substituting the random synapse formation with the Model of Structural Plasticity. As a homeostatic model, neurons regulate their own activity by growing and pruning of synaptic elements based on their current activity. Utilizing synapse formation with respect to the Euclidean distance between the neurons with a scalable algorithm allows us to easily simulate 4 million neurons with 343 memory engrams. These engrams do not interfere with one another by default, yet we can change the simulation parameters to form long-reaching associations. Our model paves the way for simulations addressing further inquiries, ranging from memory chains and hierarchies to complex memory systems comprising areas with different learning mechanisms.

Author summary

Memory is usually explained by the strengthening or weakening of synapses that fire closely after each other. This limits the forming of memory to already connected neurons. Recent work showed that memory engrams can be formed with structural plasticity on a homeostatic base. In this model, the synapses of neurons have a fixed weight, and the model forms new synapses to have sufficient synaptic input to maintain a steady fire rate. However, this model connects neurons uniformly at random, limiting the parallel formation of memories. We extend this work by using a more biologically accurate model that connects neurons in a distant-dependent manner enabling us the parallel formation of memories. The scalability of our model enables us to easily simulate 4 million neurons with 343 memories in parallel without any unwanted inference. Our model increases biological accuracy by modeling brain-like structures such as cortical columns and paving the way for large-scale experiments with memory.

Introduction

Memory is a key ingredient in our thinking and learning process. However, the understanding of learning and memories is still very limited. Already in 1921, Richard Semon described the idea of a memory engram which is the neurophysiological trace of a memory. Nowadays, working memory is usually characterized by persistent neuron activity [1]. Recent work [2] modeled this persistent activity with a partly plastic network and synaptic plasticity. However, synaptic plasticity is limited to changing the weights of already existing connections and prohibits the formation of new synapses between neurons, preventing learning relationships between these neurons. Assuming that groups of neurons represent memories, this limits learning to already connected neurons preventing learning of new relationships between unconnected neurons. Moreover, this drastically limits the storage capacity of the brain [3]. Structural plasticity can overcome both problems. Additionally, recent work showed that structural plasticity also plays an essential role in the biology of memory formation [4–6].

While most structures [7, 8] and synapses in the developed brain remain stable, there is evidence that learning [9] and sensory input leads to an increased synapse turnover, growth of dendritic spines, and axonal remodeling [10]. For example, the alternate trimming of whisker hair of mice leads to a changed sensory input and an increased dendritic spine turnover [11], with 50% of the formed spines becoming stable. Another example is the change in the gray matter of the brain when adults learn juggling [12]. Recently, it was proposed that synaptic plasticity plays a vital role in memory consolidation [5, 6, 13]. This is the process of transmitting information from the working memory into the long-term memory. First, learning increases the synaptic turnover and the formation of vacant synaptic elements [6, 9, 13]. Synaptic elements are dendritic spines or axonal boutons, which, if unoccupied, generate potential synapses [14]. Some of the potential synapses later materialize, forming new synapses [6, 13]. This hypothesis is further supported by the correlation between spine stabilization and the performance of animals in tests [15]. Moreover, when newly formed synapses during training are impaired, the performance of the animal decreases [16], indicating that the formation of new synapses is essential for learning. However, how the learning process interacts with the increased turnover and stabilization of specific spines, without overall modification of the structures in the brain, remains unclear [13].

The human cortex is organized in columns which themselves are organized in minicolumns [17]. Each of these minicolumns consists of excitatory pyramid cells that act as a group for a specific feature depending on the cortex area. For example, a minicolumn in the visual cortex represents an orientation of an object in a visual field [18]. The different minicolumns combined comprise a hypercolumn that enables encoding all orientations for a certain spot on the retina. Similar organizations can be found amongst others in the auditory cortex [19] and the somatosensory cortex [20]. The columns of higher associative cortices represent more complex features such as colors [21], objects [22], or persons [23]. We use the cortical organization of the associative cortices, where complex features can be learned and represented in a column. Hence, we split our network into boxes that represent a column. Each column represents a feature, acts independently from neighboring columns, and can therefore be active simultaneously. In our example with the visual cortex, two neighboring columns encode an orientation for their field of view, respectively, without interference.

The idea to form memory engrams based on structural plasticity was already proposed by Dammasch et al. (1990) [24]. Recently, Gallinaro et al. (2022) [25] developed a model that can form silent memory engrams with only structural plasticity on a homeostatic basis. They showed that a homeostatic rule implicitly models a Hebbian learning rule and demonstrated this principle with a conditioned learning paradigm. However, their model connects neurons uniformly at random, making the

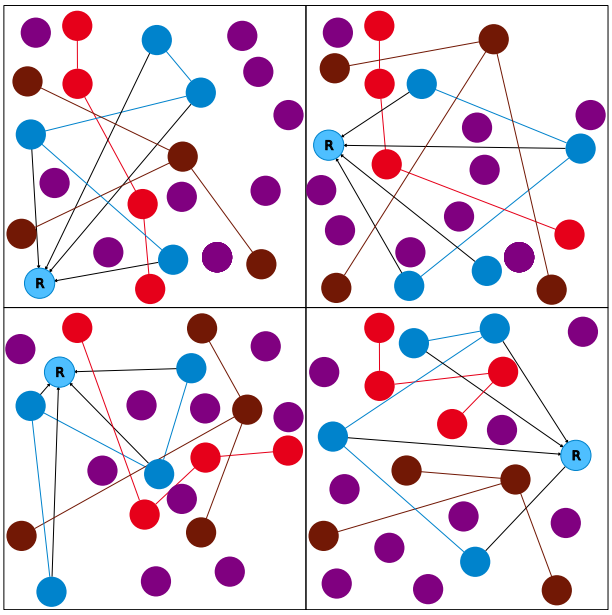

Fig 1. Setup of the network as a 2D example. We split the boxes into equally sized boxes and group a subset of neurons from each box in three equally sized ensembles representing the unconditional stimulus (US), the first conditional stimulus (C1) and the second conditional stimulus (C2). The neurons of the ensemble US are fully connected with an additional readout neuron (R). The remaining neurons do not belong to any ensemble.

simultaneous formation of clustered neurons as memory engrams impossible. The stimulation of multiple memory engrams at once would lead to one single large memory engram instead of multiple small ones but this is in contrast to the brain where different regions are active simultaneously without interfering with each other. We extend their work with a more neurophysiological accurate approach by connecting neurons depending on their distance and forming memory engrams simultaneously. We simulate 4 million neurons with 343 engrams enormously increasing the number of simulated neurons and memory engram simulated with homeostatic structural plasticity and show that the engrams do not interfere with each other.

Our results lay the foundation for modeling more complex memory systems with a large number of neurons.

Our contributions are:

- We increased the neurophysiological plausibility of homeostatic memory models, which enables us to model cortical-like structures.
- Our model maintains the introduced structure of the cortical columns without additional restraints to which the neurons can connect.
- We formed multiple ensembles in parallel without unwanted inference between them. This is comparable to the brain with its many concurrent activities.

Results

We simulated homeostatic structural plasticity between neurons with the Model of Structural Plasticity (MSP) [26]. Neurons form synaptic elements based on their

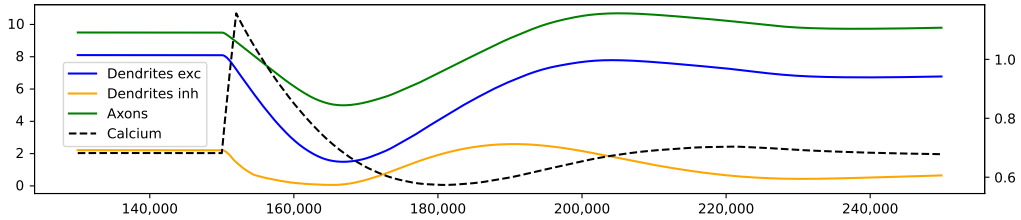

(a) Average grown synaptic elements

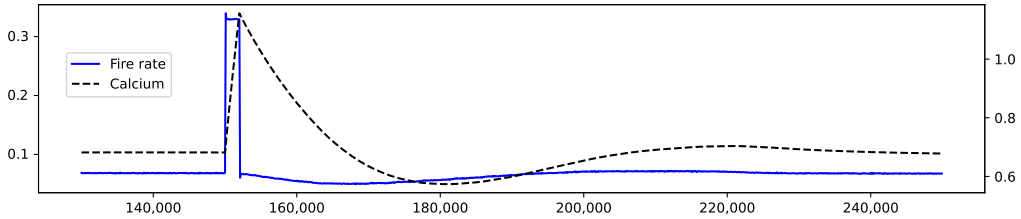

(b) Average fire rate

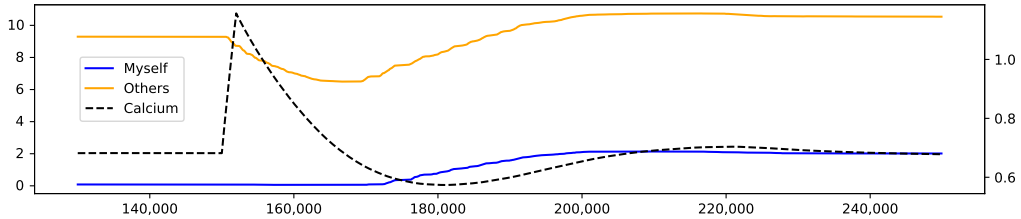

(c) Average connectivity to the ensemble itself and other neurons

Fig 2. Mechanism of a single engram formation shown with a single ensemble group US. The stimulation in step 150,000 starts the engram formation. As we see in 2b, the fire rate of the stimulated neurons increases drastically for the time of the stimulation before it falls back below its original level. With the increased fire rate, the calcium levels of the stimulated neurons increase too until it starts decreasing but slower as the fire rate. Due to the high calcium level, the neurons prune their synaptic elements until the calcium level falls below its threshold, as shown in 2a. The reduced number of synaptic elements leads to less synaptic input and, therefore, to a lower fire rate. Hence, the neuron grows synaptic elements again until the calcium level stabilizes at its set points. 2c Due to the synchronous growing of synaptic elements of the neurons within the ensemble, they connect higher than before with each other. This results in engram formation.

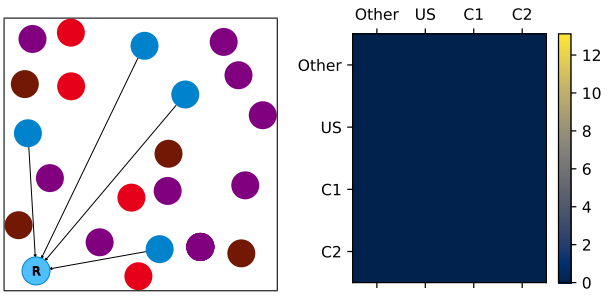

(a) At the beginning

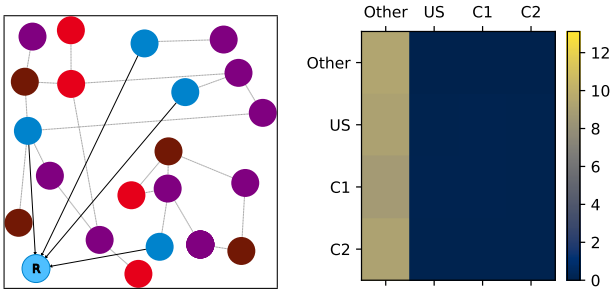

(b) After growing period

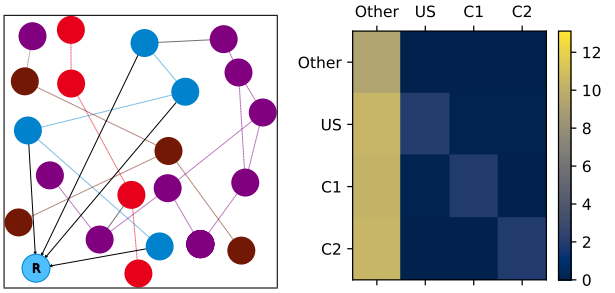

(c) After baseline phase

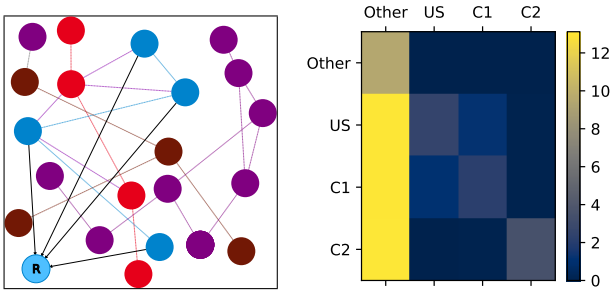

(d) After encoding phase

Fig 3. Schematic illustration of the connectivity within a single box (left) and the average number of connections from (row) to (column) a neuron in the ensemble (right). 3a. We start the simulation with only the static (solid lines) connections of US to the readout neuron and without plastic (dashed lines) connections. 3b. We start the simulation with the grown network that has random connectivity. 3c. The network shows strong connectivity within the ensembles US, C1, and C2. 3d. Additional to the strong connectivity within the ensembles, even stronger connectivity between the ensembles US and C1 is formed.

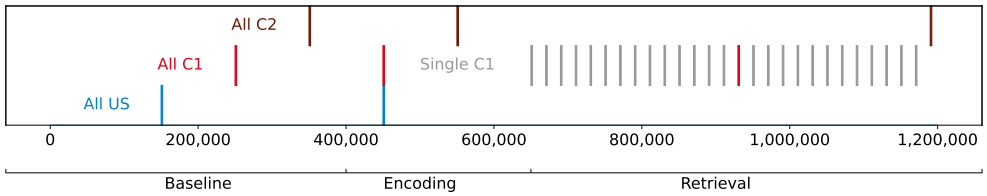

(a) Stimulation protocol of the experiment. The experiment is split into three stimulation phases: baseline, encoding, and retrieval. We stimulate the three ensemble types US, C1, and C2 after each other during the baseline phase, and stimulate US and C1 together during the encoding phase. Finally, in the retrieval phase, we stimulate the single ensembles C1 after each other. We turn the plasticity off for the retrieval phase so that earlier checks do not interfere with later checks.

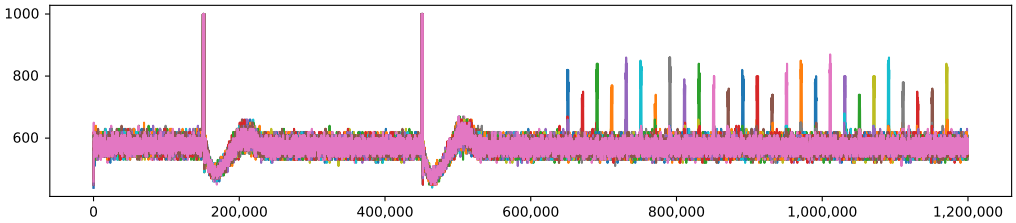

(b) Fire rates of all 27 readout neurons laid over each other

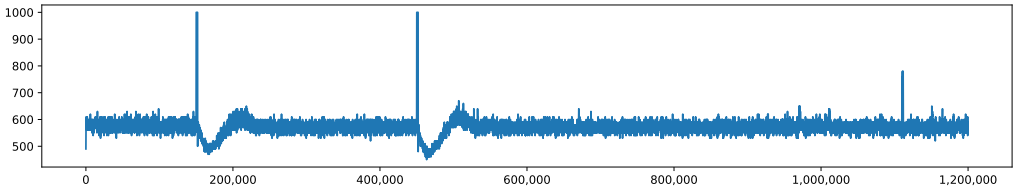

(c) Fire rate of a single readout neuron. During the retrieval phase it only fires with an increased activity when the associated C1 is stimulated.

Fig 4. Fire rates of the readout neurons. Clear spikes during the stimulation of US during the baseline phase (step 150,000) and during the stimulation of US and C1 in the encoding phase (step 450,000). During the stimulation of the single C1 ensembles in the retrieval phase, the associated readout neuron fires with a higher activity than normally but with a smaller one than during the direct stimulation of US.

intracellular calcium level that acts as a proxy for the average neuronal firing rate. If the average neuronal firing rate is below its target level, it forms new synaptic elements. If the firing rate is greater than the target level, it prunes synaptic elements. By deleting synaptic elements, causing the deletion of synapses, or by forming new synaptic elements, increasing the chance for adding new synapses, the individual neuron can regulate its own activity.

It connects unbound synaptic elements based on their distances using a two-dimensional Gaussian kernel function. We refer to Section Materials and methods for details about the Model of Structural Plasticity.

In the experiment, we followed the work of Gallinaro et al. (2022) [25], modeling a conditioned learning paradigm. In a conditioned learning paradigm, a subject learns the relationship between an unconditioned stimulus and a neutral stimulus. Before the experiment, the subject shows an unconditioned reaction to the unconditioned stimulus. During the experiment, both, unconditioned (e.g., food) and neutral stimuli (e.g., bell) are presented at the same time. After the experiment, the subject shows the same previously unconditioned (now conditioned) reaction (e.g., salivating) for the previously neutral (now conditioned) stimulus. At the level of neuronal networks, we modeled a stimulus by stimulating neurons and a reaction as the firing of a down-stream, so-called readout neuron. We split the whole population into boxes of equal side lengths and divided those neurons within each box into four distinct neuron ensembles: Unconditioned stimulus (US), conditioned stimulus 1 (C1), conditioned stimulus 2 (C2), and the rest. We add a single readout neuron (R) to each box that is fully connected to the neurons in the ensemble US with static connections (Fig. 1) to monitor the unconditioned reaction of the network. The remaining neurons do not belong to any group. With these neuron ensembles, we can model a conditioned learning paradigm by representing a neuron ensemble with a stimulus. Similar to the conditioned learning paradigm, where an unconditioned learning stimulus is presented at the same time with a conditioned stimulus and, therefore, learns a relationship between them, the network shall learn a relationship between US and C1 within each box. However, there should be no relationship associated with C2 or across different boxes. To accomplish this, we stimulate the ensembles US and C1 together.

Process of engram formation

In more detail, our stimulation protocol consists of the three phases baseline, encoding, and retrieval. We visualize our stimulation protocol in Fig. 4a. We start with the baseline phase. The goal of this phase is to form neuron ensembles with a strong within connectivity. To achieve this, we start our simulation so that the network starts forming random connections weighted based on the neuron's distances. When the network reaches an equilibrium with a stable fire rate and only minor changes in the connectivity, we stimulate a single neuron ensemble. We stimulate each neuron within the ensemble for the same duration and with the same potential. As visualized in Fig. 2, the additional stimulations results in an increased fire rate of the neurons which in consequence leads to an increase in their calcium level and therefore to a pruning of synapses. After the stimulation ends, the fire rate falls before its usual level due to the smaller synaptic input caused by the pruning of synapses. In consequence, the neurons within the ensemble start to regrow their synapses until they reach a stable fire rate and calcium level as its target value. All neurons within the ensemble regrow their synapses at the same time and are therefore looking for new synapses partner at the same time. This high ratio of potential partners within the same ensemble results in a strong connectivity within this ensemble. We stimulate a single ensemble such as US from each box at the same time. This and the property of forming new synapses based on the distance of neurons results in a strong within connectivity of this ensemble within a box.

After a short delay, we continue with the second ensembles C1 and after another delay with ensembles C2. As a result, we have three strongly within connected ensembles in each box that each represent an engram. We refer to the work of Gallinaro et all. (2022) [25] for details of this process. Fig. 3 shows the process of the reorganization of the connectivity during the entire experiment.

Next, we continue with the encoding phase. In this phase, the model learns the association between the memory ensembles US and C1 within each box. For this, we stimulate the ensembles US and C1 together. As a consequence the ensembles US and C1 in a single box form many connections using the same mechanism as in the baseline phase. We assure that the network learns only an association between US and C1 by stimulating the ensemble C2 alone as control after a delay. Similar to the baseline phase, we stimulate the specified ensemble types from each box at the same time.

Finally, in the retrieval phase, we check if the model learned the associate between US and C1. For this, we turn the plasticity off and stimulate the ensemble C1 from each box after each other while we observe the readout neurons. Note, that this is different from the previous two phases where we stimulated the same ensemble type (e.g. US) from each box at the same time. The readout neuron from each box fires with an increased activity when the ensemble C1 from the same box is stimulated as visualized in Fig. 4b. As a control, we stimulate the ensembles C2 together and assure that the readout neuron fires not with an increased activity during the control stimulation and the stimulations of ensembles from other boxes. We would expect that the readout neuron of a box fires with an increased rate, when we stimulate C1 of the same box due to the learned relationship.

Simultaneous formation of memory engrams

Our network consists of $3 \times 3 \times 3 = 27$ boxes, each with three ensembles: US, C1, and C2. By plotting the readout neurons in Fig. 4, we show that the network learns the relationships between US and C1 in each box and not between US and C2. Without stimulation, the readout neurons fire with a frequency of about 600 Hz. All readout neurons fire at steps 150,000 and 450,000 with the maximal frequency of 1000 Hz. This is followed by a decrease of the fire rate to about 450 Hz until it recovers to its normal frequency of 600 Hz. In step 150,000, during the baseline phase, we stimulate the ensembles US that are directly connected to their readout neurons. During the stimulations of C1 in step 250,000 and C2 in step 350,000, the readout neurons do not fire with an increased activity compared to their baseline frequency. This shows that the network works as desired because the unconditioned reaction is shown after the unconditioned stimulus. Later, during the encoding phase, the readout neurons fire again as expected when US and C1 are stimulated together in step 450,000 but not when C2 is stimulated in step 550,000. Finally, in the retrieval phase, we stimulate the ensemble C1 from each box after each other. We see that the readout neuron of the same box fires when its ensemble C1 is stimulated, indicating that the network learned the relationship between US and C1 only within the same box, but not beyond box boundaries. The fire rates are lower than during the stimulation in the encoding phase but still very distinguishable from the rest of the activity. We can notice small spikes of some readout neurons when another box is stimulated. A possible cause is that the ensembles are close to each other, resulting in the formation of connections beyond a single box. However, the stimulation of our control ensembles C2 still does not influence the readout neurons.

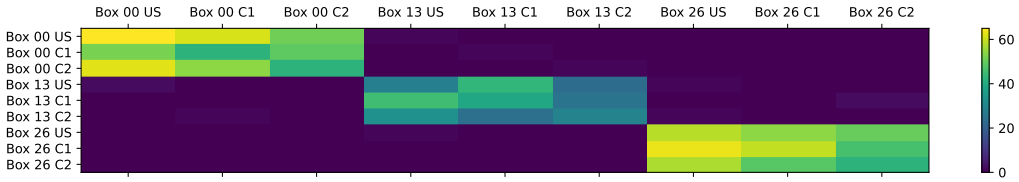

(a) Connectivity before the first stimulation during the baseline phase at step 150,00

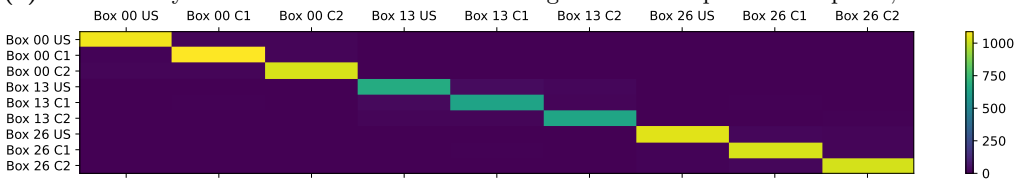

(b) Connectivity after the baseline phase at step 450,00

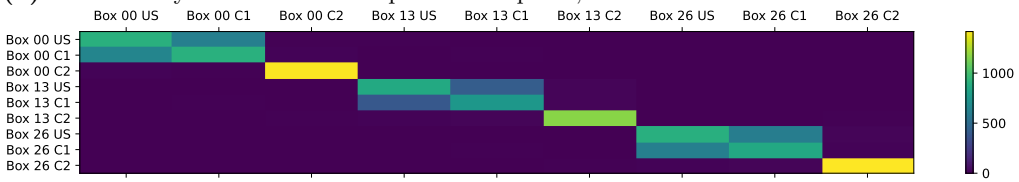

(c) Connectivity after the encoding phase at step 650,000

Fig 5. Connectivity between chosen ensembles in the network. From the top left box of the first layer (box 00) over the center box of the second layer (box 13) to the bottom right box of the last layer (box 26). a) The connectivity at the beginning of the simulation is random within a box. b) At the end of the baseline phase, the ensembles have strengthened their connections. c) After the encoding phase, the connectivity between the ensembles US and C1 within a box is very high

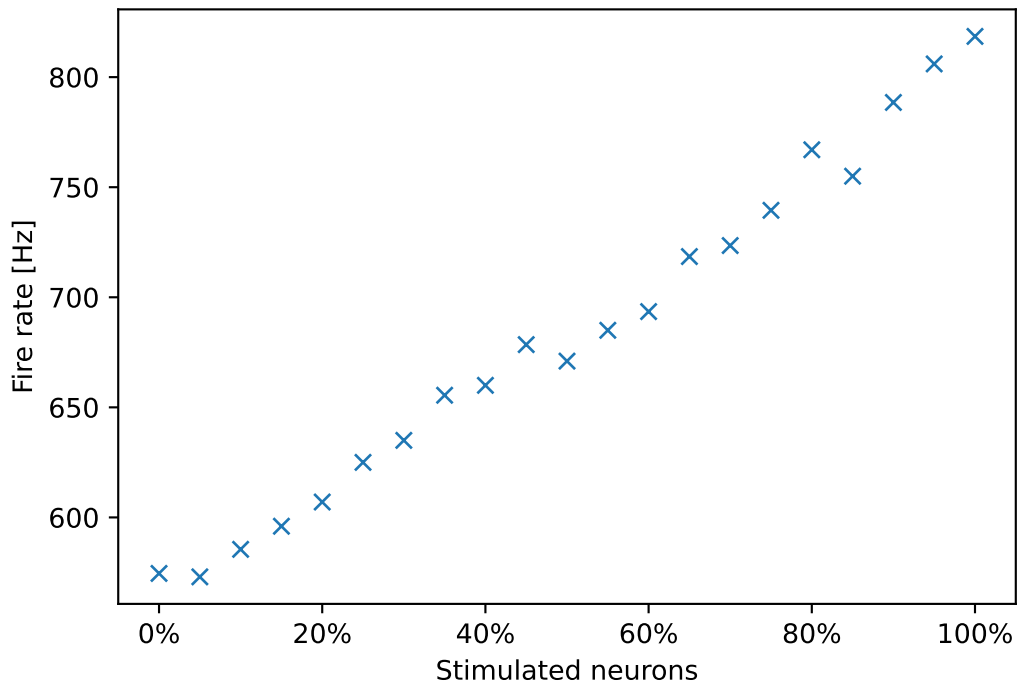

Fig 6. Fire rate during pattern retrieval. The normal fire rate of the readout neuron without any stimulation has a mean of $\mu = 574.5\,\text{Hz}$ and a standard deviation $\sigma = 29.3$. When we stimulate an increasing number of neurons in the ensemble C1, the fire rate of the readout neuron of the associated readout neuron fires with an increasing fire rate. There are three exception were an increase of the number of stimulated neurons about 5% do not increase the fire rate.

.

Large-scale formation of memory engrams

To show how well our approach scales, we successfully repeated the experiment with a larger network. Instead of $3 \times 3 \times 3 = 27$ boxes, we split a larger network into $7 \times 7 \times 7 = 343$ boxes with a total of $343 \cdot 12,500 = 4,287,500$ neurons and stimulate the network following the same pattern as before. We analyze the fire rates of the readout neurons to check whether they fire only when US is stimulated during the baseline and encoding phases and only when C1 in the same box is stimulated during the retrieval phase. Hence, we interpreted the fire rate of a readout neuron as significantly increased when it is larger than its mean and three times the standard deviation as described in Eq. 13. We assess that the network behaves correctly for 341 readout neurons firing only with a significantly increased activity when expected. Two readout neurons behave not as expected. One of the readout neurons fires only with an increased rate for 1,400 steps instead of the entire 2,000 steps of the stimulation of the associated ensemble C1 during the retrieval phase. In contrast, the other readout neuron fires with an increased rate for 500 steps during the retrieval phase when another ensemble C1 is stimulated.

Pattern completion

Gallinaro et al. (2022) [25] showed that the stimulation of 50% of the neurons of a single engram was necessary to increase the activity of the rest of the engram; we will improve upon that in both the necessary threshold and the technical contribution. While we stimulated all neurons of the ensemble C1 during the retrieval in the previous

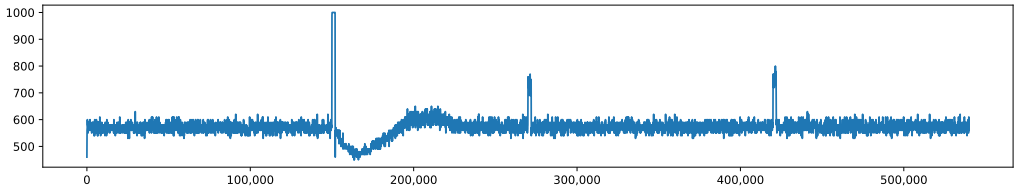

(a) Fire rate of the top left box on the top side of the cubic simulation box

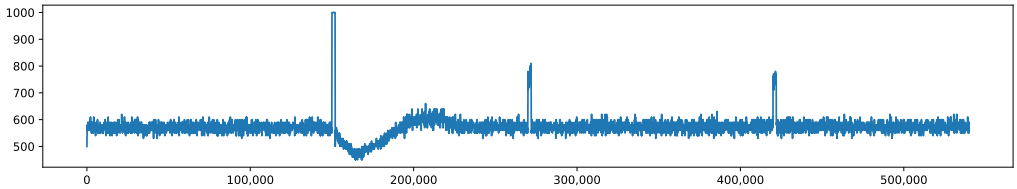

(b) Fire rate of the right bottom box the bottom side of the cubic simulation box

Fig 7. Fire rates of the two readout neurons that boxes are stimulated to form long-distance connections. Both neurons fire at a rate of 1 kHz when both ensembles are stimulated together. They fire also both when only a single ensemble C1 is stimulated indicating that both boxes form a new engram.

experiment, we now show that it is sufficient to stimulate only a subgroup of neurons in the ensemble C1 to trigger the readout neuron in the associated ensemble US. Hence, we continue simulating the network after the previous learning experiment with 27 boxes, pick a single ensemble C1 from one box, and stimulate varying numbers of neurons. As we see in Fig. 6, the fire rate of the corresponding readout neuron of US increases with more stimulated neurons of C1 except for the change between 0% – 5%, 45% – 50%, and 80% – 85% where the fire rate decreases slightly. We consider a fire rate larger than three times higher than its mean as significantly different from its baseline, as 99.7% of the baseline activity lays within this interval (3 σ rule [27]). This is the case for 45% and more stimulated neurons of the ensemble concluding that at least 150 stimulated neurons are necessary to increase the fire rate of the readout neuron significantly.

Therefore, it is enough to stimulate 20% of the neurons of the ensemble C1 to significantly reactivate the pattern so that the readout neurons fires with a significantly increased fire rate. This shows that we can also perform pattern completion over the engram pairs C1 and US due to our high connectivity within a box.

Forming long-distance connections

As described in Eq. 8 we can control the probability with which neurons connect by adjusting the Gaussian scaling parameter σ. We can connect engrams of different boxes when we increase this scaling parameter after we have already formed engrams within a box. For it, we increase σ and stimulate the ensembles US and C1 from two boxes together and check in the retrieval phase whether they form a single, interconnected engram. The fire rates are visualized in Fig. 7. We can see that the readout neuron of both boxes fire once we stimulate them together in step 150,000 and during retrieval when the C1 ensembles of both boxes are stimulated at different times. Thus, we can connect engrams that were not associated before and are distant from each other.

Discussion

We showed that the property of the Model of Structural Plasticity enables the simultaneous formation of memory engrams. We see clear, distinct spikes during the

retrieval phase, indicating that the network learned the relationship between the ensembles US and C1, although the fire rate of the readout neuron is lower than during the direct stimulation of US with 1 kHz. Moreover, while confirming the general neurophysiological conclusions of Gallinaro et al. (2022) [25], we demonstrated them at a much grander scale – with a network of 4,287,500 neurons and 343 ensemble pairs. And given the favorable scaling properties of the underlying algorithm, we see no obvious limit to further increases.

The learned relationship between US and C1 in each box can be explained with the newly formed connections as visualized Fig. 5. At the beginning of the simulation, all ensembles are randomly connected. After the baseline phase, the connectivity within the ensembles increase, and the connectivity between different ensembles decreases. This increased connectivity within ensembles indicates the formation of memory engrams similar to Gallinaro et al. (2022) [25], although we stimulated all US and C1 ensembles together only once instead of three times in a row, as they did. After the encoding phase, the connectivity between the ensembles US and C1 in the same box increases significantly, clarifying that the network learned the relationship between US and C1. However, we can see a slightly increased connectivity between the ensembles of neighboring boxes due to the connectivity probability being based on the distance of neurons. This explains the slightly increased activity of the readout neurons sometimes when another box is stimulated. Furthermore, the ensembles C2 mostly form connections within their ensembles and do not connect to neurons in other boxes or ensembles, confirming that these control ensembles do not influence the learning process.

One advantage of forming synapses, depending on the distance of the neurons, is the increased neurophysiological accuracy. In the human brain, neurons do not connect uniformly at random throughout the entire brain. Hence, the MSP connects them in a distant-dependent manner. In our model, this property enables the simulation of ongoing neuron activity in different areas of the brain without interference. Without this property, all of our ensembles US and C1 would connect to each other, forming a single large memory engram instead of various small ones. Nevertheless, engrams can be largely distributed over the brain. The adaption of the Gaussian scaling parameter σ enables simulating this behavior when desired. Through the variation of this parameter, we can allow the network to form distributed memory engrams. An increment of σ would be comparable with a phase in which the subject learns a new concept and, therefore, the plasticity in the brain increases. This could be comparable to the release of proteins during learning phases that allow higher plasticity in the brain [28, 29]. Another possibility is to model different types of neurons with different σ to ensure that some neurons can project into other brain areas while others project only locally to its direct neighbors.

Our organization in boxes is comparable with the columnar organization of the cortex. One concept is learned within a single box representing a single column comparable to the associative cortices in the brain. However, our model is still able to learn relationships between more than one box. These memory engrams do not influence the already existing local memory engrams within a box which is comparable to the human brain where inactive memories remain unchanged while non-associated memories are active. While our model learns only one pattern per box, it should be possible to learn multiple patterns in a single box with a delay. This should be possible because the formed silent memory engrams are encoded by connections and not activity enabling forming of additional memory engrams with the remaining neurons. The effect on the already formed memory engrams should be minor. Furthermore, a reduction of the number of neurons within ensemble could increase the storage capacity of a single box further. This increased storage capacity would increase further the biological plausibility, in contrast to the rather inefficient usage of neurons in our model.

Another view on our model is its similarity to the hippocampus that is an essential area in memory formation [30] and shows structural changes during learning [31–33]. Declarative memory and spatial memory is often associated with the hippocampus [34–36]. Spatial memory and enables us to navigate and capture the relation of locations. It was originally suspected that the brain consists of a spatial allocentric map that would allow a mapping of locations in an absolute coordinate system [37–39] but newer research discarded this idea [40]. Nevertheless, place cells have been found in the hippocampus of humans and rats that are active when the subject is at a certain location [40–44]. These place cells allow a reliable detection of the location but are not spatially distributed in the hippocampus. However, place cells of the same or nearby location tend to cluster [45] and distances between these place cells correlate to their represented real world locations [46]. Neurons that represent similar concepts such as similar locations are often located close to each other. Other examples can be found in the cortex from the retinotopic organization of the visual cortex [18, 47], the cerebral cortex [48]. This is similar to our model where engrams are more likely to form locally leading to a clustering of neurons forming an engram. In our model, one box represents a concept comparable to a place field. With our simulation, we could show that it is possible to form these place cells by simultaneous stimulation comparable to long-term potentation [49]. When rats were placed in a new environment within minutes new place cells were activated in the hippocampus and recruited so that they could be recalled weeks later [50, 51]. Our model explains this process through the increased activity of the neurons which leads to a locally limited cluster formation. Only a small cue such as a perceived environmental one or the recall of the location in the imagination can reactivate the cluster of place cells [52]. This is similar to our model where only a partial activation of the unconditioned stimulus (similar to an environmental cue) leads to the reactivation of the conditioned stimulus.

While memory is usually associated with synaptic plasticity, structural plasticity can explain the information storage capacity of the brain. If we consider only synaptic plasticity in the memory formation process, we are limited to forming memories with neurons that have already formed connections. Besides suffering from limited storage capacity and the necessity to maintain weak but useless synapses between unrelated neurons, associations between two memory engrams that are not connected to each other cannot be learned. Structural plasticity can overcome this limitation and enables us to simulate multiple memory engrams at the same time. Moreover, the information storage capacity can be increased by recruiting neurons to more than one ensemble. This can explain how the human brain can learn a high number of concepts and associations with a limited number of neurons. In our simulations, neurons are, for the most part in a single memory engram, but forming multiple memory engrams in a single box with overlapping neurons could significantly increase the number of engrams that can be simulated with the same number of neurons.

We believe that our approach lays the foundation for more complex memory systems. As we have demonstrated, we can form engrams locally within a box as well as over longer distances by adapting the Gaussian scaling parameter σ. Besides the already discussed recruiting of neurons in multiple engrams, we could build associations between multiple engrams locally or distribute them across the network. This would be an important extension because memories in the brain do not exists in a single one to one relationship, but rather in dependence of many other memories. Another possibility is to build a memory hierarchy with directed associations where one memory engram activates another but not the other way around. In that case an abstract concept represented as a memory engram is more strongly associated with another than the other way around. A combination of these extensions would enable the building of a more complex memory system.

Materials and methods

Izhikevich model

We chose the Izhikevich model [53] as our neuron model because it enables modeling different spiking patterns and strikes a good compromise between biological accuracy and computational efficiency. We describe the membrane potential in Eq. 1 where k_0, k_1, and k_2 are constants and u is the membrane recovery variable as described in Eq. 2. The membrane recovery depends on the fixed parameters a, b, and c and accounts for the hyperpolarization period of a neuron. Finally, we assume that a neuron spikes if the membrane potential reaches $30\,\mathrm{mV}$. Then, we reset the membrane potential and membrane recovery variables according to Eq. 3.

$$\frac{dv}{dt} = k_2 v^2 + k_1 v + k_0 - u \tag{1}$$

$$\frac{du}{dt} = a(bv - u) \tag{2}$$

$$\text{if } v \geq 30\,\mathrm{mV}, \text{then} \begin{cases} v \leftarrow c \\ u \leftarrow u + d \end{cases} \tag{3}$$

Model of Structural Plasticity

The Model of Structural Plasticity (MSP) [26] enables structural plasticity based on a homeostatic mechanism. Each neuron controls its own excitability and, therefore, the number of synapses based on its calcium concentration that acts as a proxy for its fire rate. An approximation of MSP [54, 55] reduced the model's computational complexity from $\mathcal{O}(n^2)$ to $\mathcal{O}(n \log n)$, which enabled simulations with up to 10^9 neurons. Using current technology, human-scale simulations with 10^{11} neurons are possible in principle. The MSP was recently extended with an approximation that significantly reduces the model's computational complexity and enables the simulation with the number of neurons in the human brain [54]. We provide all model parameters in Tab. 1.

Growth model

$$\frac{d\mathrm{Ca}}{dt} = \begin{cases} \frac{-\mathrm{Ca}}{\tau} + \beta & \text{if neuron fires} \\ \frac{-\mathrm{Ca}}{\tau} & \text{otherwise} \end{cases} \tag{4}$$

The calcium concentration that acts as a proxy for the fire rate is described in Eq. 4. It decreases over time with the time constant τ and increases by β when the neuron fires. Based on the calcium concentration, the number of synaptic elements of a neuron grows or shrinks by z, as described in Eq. 5. It depends on the growth rate ν, the current calcium concentration Ca, the minimum calcium concentration η required to grow synaptic elements, and the target calcium rate ϵ. Hence, if the calcium concentration is higher than the target, the neuron prunes synaptic elements, and it grows new elements if the concentration is lower than the target. We follow Butz et al. (2013) [26] for selecting our minimum calcium concentration η_{axon}, $\eta_{\mathrm{den_ex}}$, and $\eta_{\mathrm{den_inh}}$, where they showed that a high η_{axon} and a low η_{den} matches the experimental data and enables functional remapping.

$$\frac{dz}{dt} = \nu \left(2 \cdot \exp\left(-\left(\frac{\mathrm{Ca} - \xi}{\zeta} \right)^2 \right) - 1 \right) \tag{5}$$

$$\xi = \frac{\eta + \epsilon}{2} \tag{6}$$

Parameter	Parameter description	Value
$\mu_{\text{background}}$	Mean of the background activity	5
$\sigma_{\text{background}}$	Standard deviation of the background activity	2
θ	Barnes–Hut acceptance criterion	0.3
τ_{vac}	Retract ratio	100
ϵ	Target calcium level	0.7
η_{axon}	Minimum calcium level to grow axons	0.4
$\eta_{\text{den_ex}}$	Minimum calcium level to grow excitatory dendrites	0.1
$\eta_{\text{den_inh}}$	Minimum calcium level to grow inhibitory dendrites	0
σ	Gaussian scaling parameter	12
k	Synapse conductance	3
τ	Calcium decay constant	10,000
β	Calcium intake	0.001
ν_{axon}	Growth rate of axons	0.0003
$\nu_{\text{den_ex}}$	Growth rate of excitatory dendrites	0.0006
$\nu_{\text{den_inh}}$	Growth rate of inhibitory dendrites	0.0006
a_{izh}	Izhikevich model parameter	0.1
b_{izh}	Izhikevich model parameter	0.2
c_{izh}	Izhikevich model parameter	-65
d_{izh}	Izhikevich model parameter	2

Table 1. Parameters for the experiments

$$\zeta = \frac{\eta - \epsilon}{2\sqrt{-\ln(0.5)}} \tag{7}$$

Forming and pruning of synapses

Since we already determined, how many synaptic elements a neuron forms, we must now actually form synapses between unbound synaptic elements or prune them if the number of grown synaptic elements of a neuron is smaller than its actual synapses. In the last case, we choose a synapse to prune uniformly at random from all synapses of the neuron. In consequence, the synapse will be removed on the source and target neuron independent from the number of grown synaptic elements of the partner neuron. When we need to form a new synapse, we choose a neuron randomly, where the neuron candidate j is weighted with a probability p_{ij} based on the distance between the positions of the initiating neuron x_i and the candidate's position x_j and the number of vacant synaptic elements, as described in Eq. 8. Note that the implementation uses an approximation [54, 55] so that it must not calculate the probability for all neuron candidates.

$$p_{ij} = \exp\left(\frac{||x_j - x_i||_2^2}{\sigma^2}\right) \cdot \text{vac}_j \tag{8}$$

Synaptic elements that are not connected are removed over time depending on the time constant τ_{vac}, as described in Eq. 9.

$$\frac{d\text{vac}}{dt} = -\frac{\text{vac}}{\tau_{\text{vac}}} \tag{9}$$

Electrical activity

The electrical input I is the sum of three inputs: synaptic, background, and stimulation, as described in Eq. 10. The synaptic input (Eq. 11) is the sum of all fired input neurons

j. The weight is either 1 for excitatory input neurons or -1 for inhibitory ones. Moreover, the weight is multiplied by the fixed synapse conductance k. Additionally, the neurons are driven by a random, normally distributed background activity (Eq. 12).

$$I = I_{\text{synaptic}} + I_{\text{background}} + I_{\text{stimulation}} \tag{10}$$

$$I_{\text{synaptic}} = \sum_j k * w_j \tag{11}$$

$$I_{\text{background}} \sim \mathcal{N}(\mu, \sigma^2) \tag{12}$$

Network setup and stimulation

Our network consists – unless noted otherwise – of 337,500 neurons, each with a ratio of inhibitory to excitatory neurons of 20%. The positions of the neurons are equally distributed in a 3-dimensional cubic space. We split the network into 27 equally sized cubes with about 12,500 neurons each, following Gallinaro et al. (2022) [25]. In each box, we group a part of the neurons into disjoint ensembles of 333 excitatory neurons, selecting them randomly from all neurons in the box. Figure 1 visualizes the setup as a 2D example.

We start our network in a fully disconnected state and let it build up the connectivity from scratch for 1,000,000 steps until it reaches an equilibrium. We store the newly formed network and use it as a starting point for our experiment. Hence, we continued the simulation with this network and waited for 150,000 steps until the network stabilized itself.

Then, we continue the simulation with three stimulation phases similar to Gallinaro et al. (2022) [25]: baseline, decoding, and retrieval. We perform all stimulations for 2,000 steps with 20 mV. In the baseline phase, we stimulate all ensembles US in step 150,000, followed by all ensembles C1 (250,000), and lastly, all ensemble C2 (350,000). Note that US, C1, and C2 are stimulated after each other, but all ensembles of the same type are stimulated at the same time. Then, in the decoding phase, we stimulate all US and C1 ensembles together in step 450,000 and all C2 ensembles in step 550,000. Later, in the retrieval phase, we turn the plasticity off so that no further modifications in terms of creating or pruning any connections, is possible. We do this to see how the networks behave without any further modifications. Here, we stimulate, beginning in step 650,000, all C1 ensembles consecutively in isolation, one after the other, with a pause of 18,000 steps between them. In the end, we stimulate all C2 ensembles together at step 1,190,000.

Validity check

We check the fire rate of the readout neuron to ensure that the network behaves as expected. We assume that the fire rates follow a normal distribution and detect an abnormal behavior of the readout neuron when its fire rate significantly outside of the normal distribution. For it, we use the 3-σ rule [27], as described in Def. 13 with f as the fire rate of the readout neuron, μ as its mean, and σ its standard deviation without any stimulation. 99.7% of the normal fire rate lies within the interval of three times of the standard deviation around the mean of the normal distribution of the fire rate. We consider a fire rate outside of this interval for at least 500 steps as significantly different from the normal fire rate of the neuron when the network is in an unifluenced state.

$$
\begin{aligned}
f &\in [-\infty, \mu - 3\sigma) && \text{Significantly decreased fire rate} \\
f &\in [\mu - 3\sigma, \mu + 3\sigma] && \text{Normal fire rate} \\
f &\in (\mu + 3\sigma, \infty] && \text{Significantly increased fire rate}
\end{aligned} \tag{13}
$$

We expect a readout neuron to fire with an increased activity if and only if

- We stimulate its ensemble US during the baseline phase, or
- We stimulate its ensembles US and C1 during the encoding phase, or
- We stimulate its ensemble C1 during the retrieval phase

We allow the increased fire rate to start (end) within of 100 ms of the start (end) of the associated stimulation to allow for some variation in the neurons behavior.

Advanced simulations

The following two experiments start with the network that was stimulated as described in Section Network setup and stimulation because they analyze the newly created engrams.

Pattern completion

We want to see if our network can reactivate the learned pattern if we stimulate it only partly. For it, we continue the simulation and wait for 60,000 steps until the network stabilizes. Then, we stimulate 5% randomly chosen neurons of the ensemble C1 of the center box for 2,000 steps. After a pause of 98,000 steps, we add a further 5% randomly chosen neurons of the ensemble to the stimulated neurons and stimulate again. We repeat this cycle until we stimulate 100% of the ensemble.

Forming long-distance connections

During our main experiment, we wanted to build memory engrams only within a box. Now, we want to show that we can still form connections over long-distances and therefore combine memory engrams from different regions. For it, we we continue the simulation with a larger Gaussian scaling parameter σ_{distant} that makes connections over long-distances more probable. We select two edge boxes on the opposite side of the simulation area to maximize the distance. We wait for 150,000 steps so that the network can stabilize first. Then, we stimulate the ensembles US and C1 from both boxes together for 2,000 steps. After a pause, we turn the plasticity off in step 250,000 and stimulate each ensemble C1 from each box after each other with a pause of 8,000 steps between them to check if the network learned the relationship between the ensembles in the two boxes without interfering with other boxes. As a last stimulation in step 520,000, all of the ensembles C2 are stimulated to check the response to the control ensembles.

Supporting information

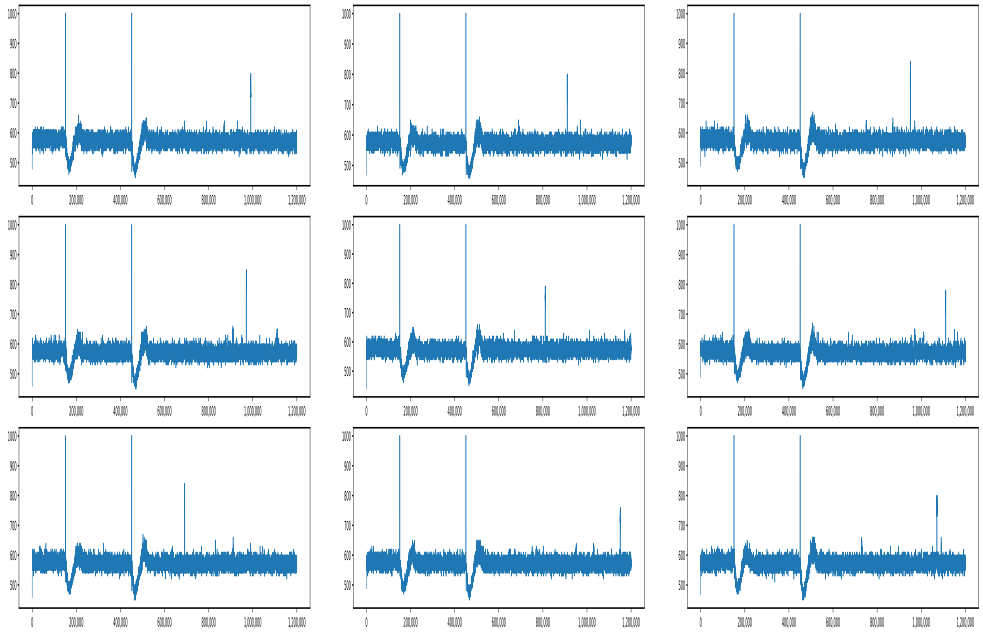

(a) First layer with 9 out of 27 boxes.

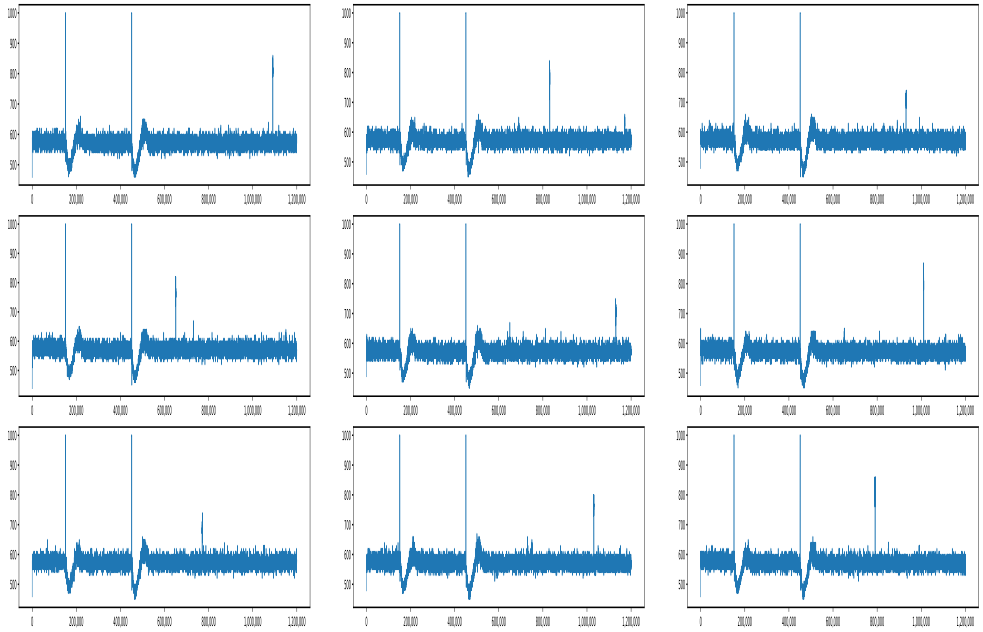

(b) Second layer with 9 out of 27 boxes

Fig 8. Separate visualization of all 27 readout neurons spatially organized.

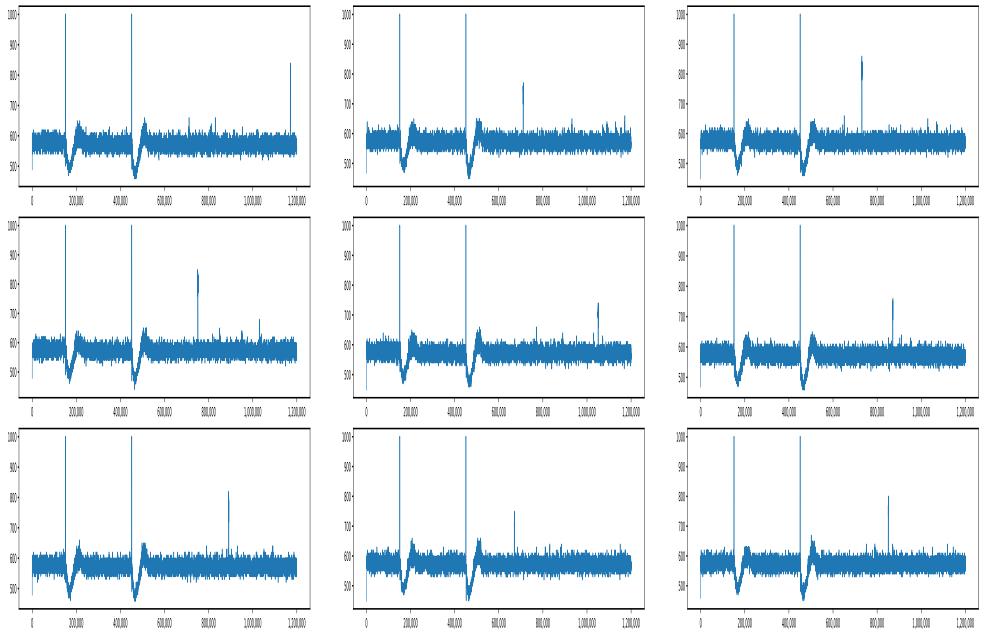

(c) Last layer with 9 out of 27 boxes

Fig 8. Separate visualization of all 27 readout neurons spatially organized.

References

1. Barak O, Tsodyks M. Working models of working memory. Current Opinion in Neurobiology. 2014;25:20–24.
2. Fiebig F, Lansner A. A Spiking Working Memory Model Based on Hebbian Short-Term Potentiation. Journal of Neuroscience. 2017;37(1):83–96.
3. Chklovskii DB, Mel BW, Svoboda K. Cortical rewiring and information storage. Nature. 2004;431.
4. May A. Experience-dependent structural plasticity in the adult human brain. Trends in Cognitive Sciences. 2011;15:475–482.
5. Holtmaat A, Caroni P. Functional and structural underpinnings of neuronal assembly formation in learning. Nature Neuroscience. 2016;19:1553–1562.
6. Butz M, Wörgötter F, Ooyen AV. Activity-dependent structural plasticity. Brain Research Reviews. 2009;60:287–305.
7. Mizrahi A. Dendritic development and plasticity of adult-born neurons in the mouse olfactory bulb. Nature neuroscience. 2007;10(4):444–452.
8. Kalisman N, Silberberg G, Markram H. The neocortical microcircuit as a tabula rasa. Proceedings of the National Academy of Sciences. 2005;102(3):880–885.
9. Holtmaat A, Svoboda K. Experience-dependent structural synaptic plasticity in the mammalian brain. Nature Reviews Neuroscience. 2009;10:647–658.
10. Barnes SJ, Finnerty GT. Sensory experience and cortical rewiring. The Neuroscientist. 2010;16(2):186–198.

11. Trachtenberg JT, Chen BE, Knott GW, Feng G, Sanes JR, Welker E, et al. Long-term in vivo imaging of experience-dependent synaptic plasticity in adult cortex. Nature. 2002;420(6917):788–794.

12. Boyke J, Driemeyer J, Gaser C, Büchel C, May A. Training-Induced Brain Structure Changes in the Elderly. Journal of Neuroscience. 2008;28(28):7031–7035.

13. Caroni P, Donato F, Muller D. Structural plasticity upon learning: regulation and functions. Nature Reviews Neuroscience. 2012;13(7):478–490.

14. Stepanyants A, Hof PR, Chklovskii DB. Geometry and Structural Plasticity of Synaptic Connectivity. Neuron. 2002;34(2):275–288.

15. Xu T, Yu X, Perlik AJ, Tobin WF, Zweig JA, Tennant K, et al. Rapid formation and selective stabilization of synapses for enduring motor memories. Nature. 2009;462(7275):915–919.

16. Hayashi-Takagi A, Yagishita S, Nakamura M, Shirai F, Wu YI, Loshbaugh AL, et al. Labelling and optical erasure of synaptic memory traces in the motor cortex. Nature. 2015;525(7569):333–338.

17. Mountcastle VB. The columnar organization of the neocortex. Brain: a journal of neurology. 1997;120(4):701–722.

18. Hubel DH, Wiesel TN. Receptive fields, binocular interaction and functional architecture in the cat's visual cortex. The Journal of physiology. 1962;160(1):106.

19. Reale RA, Imig TJ. Tonotopic organization in auditory cortex of the cat. Journal of Comparative Neurology. 1980;192(2):265–291.

20. Ruben J, Schwiemann J, Deuchert M, Meyer R, Krause T, Curio G, et al. Somatotopic organization of human secondary somatosensory cortex. Cerebral cortex. 2001;11(5):463–473.

21. Hadjikhani N, Liu AK, Dale AM, Cavanagh P, Tootell RB. Retinotopy and color sensitivity in human visual cortical area V8. Nature neuroscience. 1998;1(3):235–241.

22. López-Aranda MF, López-Téllez JF, Navarro-Lobato I, Masmudi-Martín M, Gutiérrez A, Khan ZU. Role of layer 6 of V2 visual cortex in object-recognition memory. Science. 2009;325(5936):87–89.

23. Downing PE, Peelen MV. The role of occipitotemporal body-selective regions in person perception. Cognitive neuroscience. 2011;2(3-4):186–203.

24. Dammasch IE. Structural realization of a Hebb-type learning rule. In: Cotterill RMJ, editor. Models of Brain Function. Cambridge: Cambridge University Press; 1990. p. 539–552.

25. Gallinaro JV, Gašparović N, Rotter S. Homeostatic control of synaptic rewiring in recurrent networks induces the formation of stable memory engrams. PLoS Computational Biology. 2022;18.

26. Butz M, van Ooyen A. A Simple Rule for Dendritic Spine and Axonal Bouton Formation Can Account for Cortical Reorganization after Focal Retinal Lesions. PLoS Computational Biology. 2013;9:39–43.

27. Pukelsheim F. The Three Sigma Rule. The American Statistician. 1994;48(2):88–91.

28. Lamprecht R, LeDoux J. Structural plasticity and memory. Nature Reviews Neuroscience. 2004;5(1):45–54.

29. Poo Mm. Neurotrophins as synaptic modulators. Nature reviews neuroscience. 2001;2(1):24–32.

30. Squire LR, Stark CEL, Clark RE. The medial temporal lobe. Annual Review of Neuroscience. 2004;27(1):279–306.

31. Leuner B, Falduto J, Shors TJ. Associative memory formation increases the observation of dendritic spines in the hippocampus. Journal of Neuroscience. 2003;23(2):659–665.

32. Leuner B, Gould E. Structural plasticity and hippocampal function. Annual review of psychology. 2010;61:111–140.

33. Groussard M, La Joie R, Rauchs G, Landeau B, Chetelat G, Viader F, et al. When music and long-term memory interact: effects of musical expertise on functional and structural plasticity in the hippocampus. PLoS One. 2010;5(10):e13225.

34. Eichenbaum H, Cohen NJ. Can we reconcile the declarative memory and spatial navigation views on hippocampal function? Neuron. 2014;83(4):764–770.

35. Deuker L, Bellmund JL, Navarro Schröder T, Doeller CF. An event map of memory space in the hippocampus. eLife. 2016;5:e16534.

36. Eichenbaum H. On the Integration of Space, Time, and Memory. Neuron. 2017;95(5):1007–1018.

37. O'Keefe J. An allocentric spatial model for the hippocampal cognitive map. Hippocampus. 1991;1(3):230–235.

38. Tolman EC. Cognitive maps in rats and men. Psychological review. 1948;55(4):189.

39. O'keefe J, Nadel L. Précis of O'Keefe & Nadel's The hippocampus as a cognitive map. Behavioral and Brain Sciences. 1979;2(4):487–494.

40. Eichenbaum H, Dudchenko P, Wood E, Shapiro M, Tanila H. The hippocampus, memory, and place cells: is it spatial memory or a memory space? Neuron. 1999;23(2):209–226.

41. O'Keefe J, Dostrovsky J. The hippocampus as a spatial map: preliminary evidence from unit activity in the freely-moving rat. Brain research. 1971;.

42. Hill AJ, Best PJ. Effects of deafness and blindness on the spatial correlates of hippocampal unit activity in the rat. Experimental neurology. 1981;74(1):204–217.

43. Thompson L, Best P. Place cells and silent cells in the hippocampus of freely-behaving rats. Journal of Neuroscience. 1989;9(7):2382–2390.

44. Moser EI, Kropff E, Moser MB. Place cells, grid cells, and the brain's spatial representation system. Annu Rev Neurosci. 2008;31:69–89.

45. Eichenbaum H, Wiener SI, Shapiro M, Cohen N. The organization of spatial coding in the hippocampus: a study of neural ensemble activity. Journal of Neuroscience. 1989;9(8):2764–2775.

46. O'Keefe J, Burgess N. Geometric determinants of the place fields of hippocampal neurons. Nature. 1996;381(6581):425–428.

47. Tusa R, Rosenquist A, Palmer L. Retinotopic organization of areas 18 and 19 in the cat. Journal of Comparative Neurology. 1979;185(4):657–678.

48. Penfield W, Rasmussen T. The cerebral cortex of man; a clinical study of localization of function. Journal of the American Medical Association. 1950;144(16):1412–1412.

49. Teyler TJ, DiScenna P. Long-term potentiation. Annual review of neuroscience. 1987;10(1):131–161.

50. Rotenberg A, Mayford M, Hawkins RD, Kandel ER, Muller RU. Mice expressing activated CaMKII lack low frequency LTP and do not form stable place cells in the CA1 region of the hippocampus. Cell. 1996;87(7):1351–1361.

51. Lever C, Wills T, Cacucci F, Burgess N, O'Keefe J. Long-term plasticity in hippocampal place-cell representation of environmental geometry. Nature. 2002;416(6876):90–94.

52. O'Keefe J, Conway DH. Hippocampal place units in the freely moving rat: why they fire where they fire. Experimental brain research. 1978;31:573–590.

53. Izhikevich EM. Which model to use for cortical spiking neurons? IEEE Transactions on Neural Networks. 2004;15(5):1063–1070.

54. Rinke S, Butz-Ostendorf M, Hermanns MA, Naveau M, Wolf F. A scalable algorithm for simulating the structural plasticity of the brain. Journal of Parallel and Distributed Computing. 2018;120:251–266.

55. Czappa F, Geiß A, Wolf F. Simulating Structural Plasticity of the Brain more Scalable than Expected. Journal of Parallel and Distributed Computing. 2023;171:24–27.